Morphological differences in skeletal muscle atrophy of rats with motor nerve and/or sensory nerve injury★

Lei Zhao[1], Guangming Lv[2], Shengyang Jiang[3], Zhiqiang Yan[4], Junming Sun[3], Ling Wang[3], Donglin Jiang[3]

1 Department of Orthopedics, Third Affiliated Hospital of Nantong University, Wuxi 214041, Jiangsu Province, China
2 Key Laboratory of Neural Regeneration of Jiangsu Province, Nantong University, Nantong 223001, Jiangsu Province, China
3 Central Laboratory, Third Affiliated Hospital of Nantong University, Wuxi 214041, Jiangsu Province, China
4 Laboratory of Mechanical Biology and Medical Engineering, Shanghai Jiao Tong University School of Medicine, Shanghai 200030, China

Abstract

Skeletal muscle atrophy occurs after denervation. The present study dissected the rat left ventral root and dorsal root at L_{4-6} or the sciatic nerve to establish a model of simple motor nerve injury, sensory nerve injury or mixed nerve injury. Results showed that with prolonged denervation time, rats with simple motor nerve injury, sensory nerve injury or mixed nerve injury exhibited abnormal behavior, reduced wet weight of the left gastrocnemius muscle, decreased diameter and cross-sectional area and altered ultrastructure of muscle cells, as well as decreased cross-sectional area and increased gray scale of the gastrocnemius muscle motor end plate. Moreover, at the same time point, the pathological changes were most severe in mixed nerve injury, followed by simple motor nerve injury, and the changes in simple sensory nerve injury were the mildest. These findings indicate that normal skeletal muscle morphology is maintained by intact innervation. Motor nerve injury resulted in larger damage to skeletal muscle and more severe atrophy than sensory nerve injury. Thus, reconstruction of motor nerves should be considered first in the clinical treatment of skeletal muscle atrophy caused by denervation.

Key Words

Research Highlights

(1) With prolonged denervation time, rats with simple motor nerve injury, sensory nerve injury or mixed nerve injury exhibited abnormal behavior, reduced gastrocnemius muscle wet weight, decreased muscle cell diameter and cross-sectional area, ultrastructural changes, as well as diminished cross-sectional area and increased acetylcholinesterase content of the motor end plate of the left gastrocnemius muscle.
(2) At the same time point, the pathological changes were most severe in the mixed nerve injury group, and mildest in the simple sensory nerve injury group.

Lei Zhao★, Master, Associate chief physician, Department of Orthopedics, Third Affiliated Hospital of Nantong University, Wuxi 214041, Jiangsu Province, China

Lei Zhao and Guangming Lv contributed equally to this work.

Corresponding author: Donglin Jiang, Master, Associate chief physician, Central Laboratory, Third Affiliated Hospital of Nantong University, Wuxi 214041, Jiangsu Province, China
jdlstar@126.com

INTRODUCTION

The peripheral nerves interact with dominant skeletal muscles. The cell signaling link between these two cell types is abnormal after peripheral nerve injury[1], which is accompanied by changes in skeletal muscle metabolism, protein decomposition and stress reactions[2-5], activation of apoptosis[6-8], evidence of apoptosis[9], and ultimately amyotrophy. The changes in muscle tissues that occur in a short period of time after denervation are reversible, but nerve regeneration is very slow and a long time is required for regenerative axons to reach target organs (skeletal muscles). A long period of denervation results in irreversible severe amyotrophy[10]. Prevention and treatment of denervation-induced skeletal muscle atrophy is attracting increased attention[11-15], but methods for simulating denervation are limited; they include dissection, ligation, clamping, traction or freezing of the brachial plexus nerve, the sciatic nerve or its branches. Although skeletal muscle atrophy after denervation has been simulated, pathological changes and manifestations after simple motor nerve or sensory nerve injury have not been fully investigated. The present study selectively dissected the ventral root, the dorsal root or the sciatic nerve to establish nerve injury models in rats, and further observed the influence of simple motor nerve or/and simple sensory nerve injury on the morphology of the rat gastrocnemius muscle.

RESULTS

Quantitative analysis of experimental animals
A total of 54 Sprague-Dawley rats were equally and randomly assigned to ventral root transection, dorsal root transection, and sciatic nerve transection groups. Four rats died due to anesthetic accident, intraoperative bleeding and postoperative infection, with a total death rate of 7.41%. Fifty-four rats were included in the final analysis following supplementation. The rats were housed separately after surgery and six were randomly selected from each group at 2, 4 and 10 weeks post injury.

Rat behavioral changes following motor nerve or/and sensory nerve injury
In the ventral root transection group, the left hind limb was unable to move, and the rat exhibited lameness. As time progressed, muscle atrophy worsened: at 10 weeks, the atrophy was moderate. From the fourth week onward, foot ulcers gradually increased, accompanied by

autotomy. The rats vocalized in response to pricking with a needle, but did not dodge. In the dorsal root transection group, the left hind limb was able to move, but the rats' gait was not concordant. As time progressed, muscle atrophy worsened: at 10 weeks, the atrophy was mild. Foot ulcers were not found, but foot swelling developed. The rats did not vocalize in response to pricking with a needle, but they stretched their legs. In the sciatic nerve transection group, the left hind limb was unable to move, and the rats were lame. As time progressed, muscle atrophy worsened: at 10 weeks, the atrophy was severe. From the third week, foot ulcers and autotomy gradually increased compared with the ventral root transection group. The rats did not vocalize or escape in response to pricking with a needle. However, the right hind limbs of all rats exhibited normal movement, with normal muscle and concordant gait, and no muscle atrophy. They vocalized and escaped the pricking with a needle on the right side.

Gastrocnemius muscle wet weight decreased in rats with motor nerve or/and sensory nerve injury
The residual muscle rate gradually decreased with increasing denervation time, and was greatest in the dorsal root transection group, followed by the ventral root transection group, and then the sciatic nerve transection group ($P < 0.01$; Table 1). The denervated gastrocnemius muscle progressively atrophied after nerve injury (Figure 1).

Table 1 Residual muscle rate of rat gastrocnemius muscle			
Group	Time post nerve injury (week)		
	2	4	10
VRT	0.58 ± 0.06^a	0.35 ± 0.10^a	0.31 ± 0.04^a
DRT	0.86 ± 0.08	0.73 ± 0.09	0.67 ± 0.11
SNT	0.56 ± 0.06^a	0.31 ± 0.05^a	0.28 ± 0.09^a
F	39.100	46.133	41.205
P	0.000	0.000	0.000

Residual muscle rate of rat gastrocnemius muscle = denervated gastrocnemius muscle wet weight/control gastrocnemius muscle wet weight. Data are expressed as mean ± SD of six rats from each group at each time point.

The multiple-sample means were compared using analysis of variance (one-way K level), and a paired comparison of means was conducted using independent two-sample t-tests. $^aP < 0.01$, *vs.* DRT group at the same time point.

VRT: Ventral root transection; DRT: dorsal root transection; SNT: sciatic nerve transection.

Gastrocnemius muscle cell diameter and cross-sectional area decreased in rats with motor nerve or/and sensory nerve injury
The gastrocnemius muscle cell diameter and

cross-sectional area progressively decreased in rats with nerve injury (Figure 2). Moreover, the cell diameter and cross-sectional area were smallest in the sciatic nerve transection group, and largest in the dorsal root transection group ($P < 0.05$ or $P < 0.01$; Table 2).

Ultrastructure of gastrocnemius muscle cells in rats with motor nerve or/and sensory nerve injury

The ultrastructure of the gastrocnemius muscle cells exhibited similar changes in each group of rats after nerve injury. With prolonged injury time, mitochondrial swelling, disorderly myofilaments and sarcomeres, shortened cristae, expanded sarcoplasmic reticulum, reduced glycogen granules, and enlarged nuclei were observed. In addition, myofilaments and sarcomeres broke, fused or disappeared, and mitochondria became vacuolated. The number of gastrocnemius muscle satellite cells increased in all rats, reached its peak value at 4 weeks, and gradually decreased thereafter. The number of muscle satellite cells was lowest in the sciatic nerve transection group, and highest in the dorsal root transection group (Figure 3).
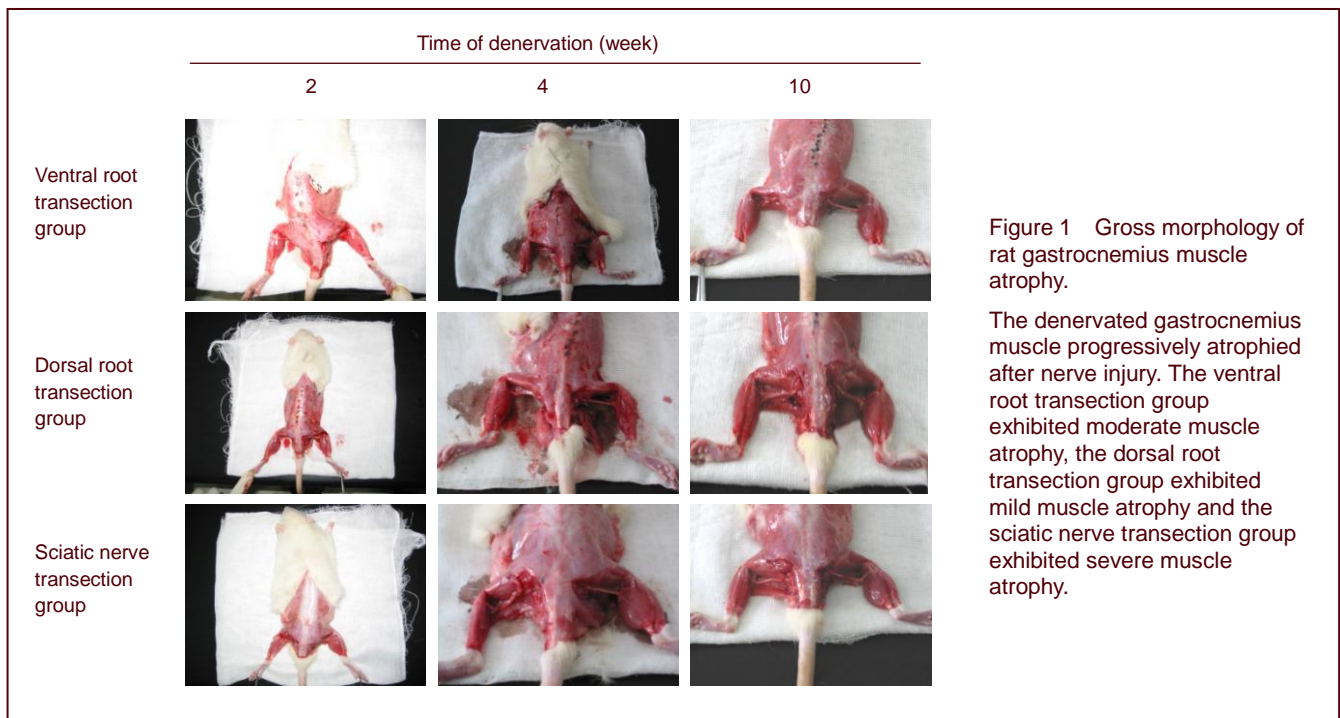

Figure 1   Gross morphology of rat gastrocnemius muscle atrophy.

The denervated gastrocnemius muscle progressively atrophied after nerve injury. The ventral root transection group exhibited moderate muscle atrophy, the dorsal root transection group exhibited mild muscle atrophy and the sciatic nerve transection group exhibited severe muscle atrophy.
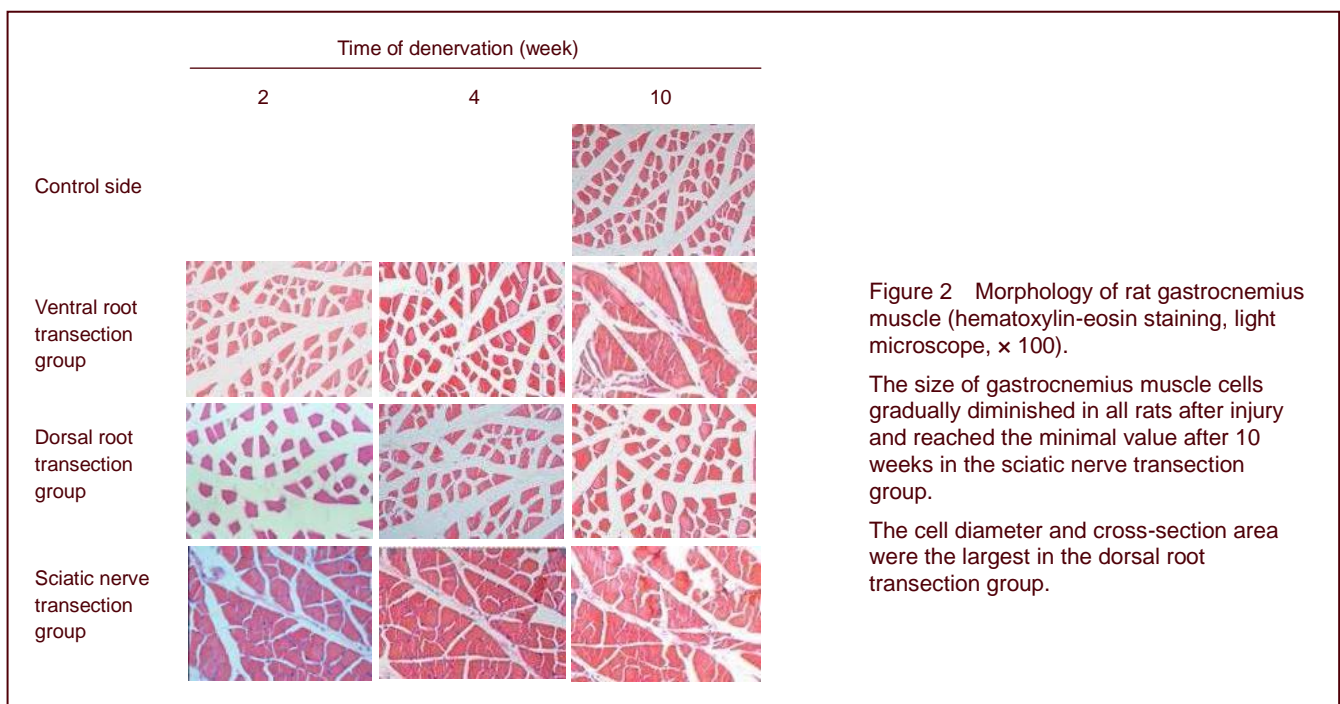

Figure 2   Morphology of rat gastrocnemius muscle (hematoxylin-eosin staining, light microscope, × 100).
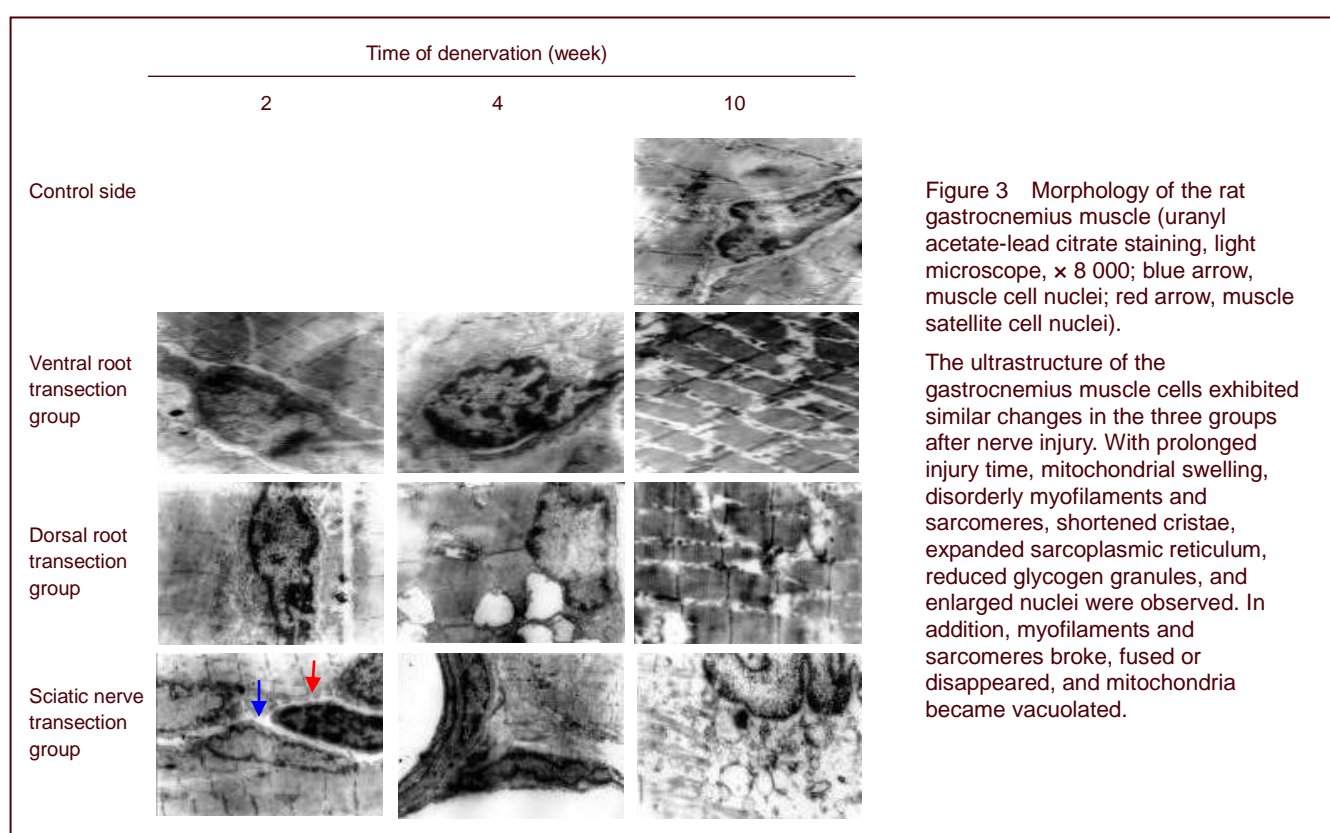
The size of gastrocnemius muscle cells gradually diminished in all rats after injury and reached the minimal value after 10 weeks in the sciatic nerve transection group.

The cell diameter and cross-section area were the largest in the dorsal root transection group.

Table 2   Cross-sectional area (μm^2) and cell diameter (μm) of gastrocnemius muscle cells

Group	2 weeks after injury		4 weeks after injury		10 weeks after injury	
	Cross-sectional area	Cell diameter	Cross-sectional area	Cell diameter	Cross-sectional area	Cell diameter
VRT	937.70±40.57[ab]	34.56±0.75[ab]	779.03±47.14[ab]	31.49±0.96[ab]	635.11±48.66[ab]	28.43±1.09[ab]
DRT	1 773.33±267.50	47.42±3.58	1 158.22±110.79[a]	38.38±1.83[a]	1 082.73±87.29[a]	37.11±1.50[a]
SNT	864.24±34.19[ab]	33.18±0.66[ab]	470.34±49.05[ab]	24.45±1.27[ab]	326.37±55.88[ab]	20.33±1.76[ab]
Control side	1 802.08±252.68	47.81±3.41	1 847.76±281.80	48.40±3.65	1 856.92±287.48	48.52±3.76
F	45.691	59.780	87.781	130.052	110.754	169.460
P	0.000	0.000	0.000	0.000	0.000	0.000

Data are expressed as mean ± SD of six rats from each group at each time point. Multiple-sample means were compared using analysis of variance (one-way K level), and paired comparison of means was conducted using independent two-sample *t*-tests. [a]$P < 0.01$, *vs.* control side; [b]$P < 0.01$, *vs.* DRT group. VRT: Ventral root transection; DRT: dorsal root transection; SNT: sciatic nerve transection.

Figure 3   Morphology of the rat gastrocnemius muscle (uranyl acetate-lead citrate staining, light microscope, × 8 000; blue arrow, muscle cell nuclei; red arrow, muscle satellite cell nuclei).

The ultrastructure of the gastrocnemius muscle cells exhibited similar changes in the three groups after nerve injury. With prolonged injury time, mitochondrial swelling, disorderly myofilaments and sarcomeres, shortened cristae, expanded sarcoplasmic reticulum, reduced glycogen granules, and enlarged nuclei were observed. In addition, myofilaments and sarcomeres broke, fused or disappeared, and mitochondria became vacuolated.

Cross-sectional area and gray scale of the motor endplate of the gastrocnemius muscle in rats with motor nerve or/and sensory nerve injury

With prolonged denervation time, the changes in motor endplate cross-sectional area and gray scale were similar in the ventral and dorsal root transection groups. The motor end plate cross-sectional area gradually decreased, but the mean gray scale gradually increased ($P < 0.01$, motor end plate cross-sectional area and gray-scale at 10 weeks *vs.* those at 2 and 4 weeks), but no changes were evident in the sciatic nerve transection group (Figure 4). Moreover, the motor end plate cross-sectional area and gray scale were similar among the three groups ($P > 0.05$), but the motor endplate cross-sectional area gradually decreased ($P < 0.01$) and the mean gray scale gradually increased ($P < 0.01$) up to 10 weeks in the ventral root transection and the sciatic nerve transection groups compared with the control side (Table 3).

DISCUSSION

The present study established an animal model of simple motor nerve or sensory nerve injury by exposing and dissecting the ventral and dorsal root at L$_{4-6}$ through the posterior intervertebral foramen. In the vertebral canal, the ventral root comprises motor fibers from the ventral

horn of the spinal cord, and the dorsal root comprises sensory fibers from the spinal dorsal horn, both of which are independent and do not overlap. This method can prevent injury to the spinal cord and adjacent nerve roots, ensuring the stability and reliability of the experimental model. Moreover, it is simple and the sample is easily available. With increasing clinical simple motor nerve or sensory nerve injury-induced diseases, such as the sequellae of poliomyelitis, muscular dystrophy, syringomyelia and Guillain-Barré syndrome, this model can provide an ideal animal model for studies of skeletal muscle regeneration and repair with a view toward future clinical treatments[16].

In the present study, as the observation time increased, muscle atrophy worsened in the ventral root transection group, accompanied by foot ulcers and autotomy; the left hind leg developed a moderate degree of atrophy up to 10 weeks. In the sciatic nerve transection group, the foot ulcers and autotomy were more serious compared with the ventral root transection group, and the atrophy developed to a severe degree up to 10 weeks. However, in the dorsal root transection group, the muscle atrophy and foot ulcers were mild, although foot swelling was observed. The wet weight of the denervated gastrocnemius, the muscle cell diameter and cross-sectional area were progressively reduced in all groups. At the same time point, the wet weight of the gastrocnemius muscle, the muscle cell diameter and cross-sectional area were smallest in the sciatic nerve transection group, greater in the ventral root transection group and greatest in the dorsal root transection group.
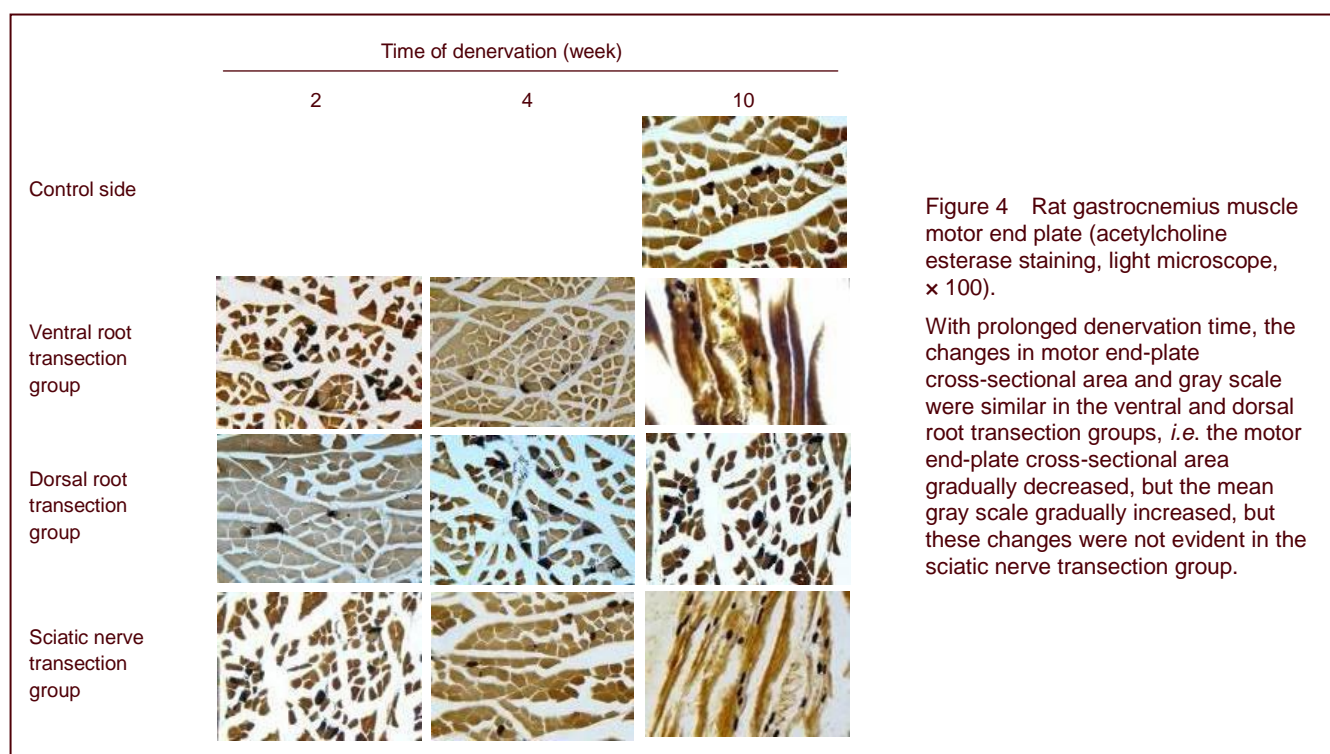

Figure 4 Rat gastrocnemius muscle motor end plate (acetylcholine esterase staining, light microscope, × 100).

With prolonged denervation time, the changes in motor end-plate cross-sectional area and gray scale were similar in the ventral and dorsal root transection groups, i.e. the motor end-plate cross-sectional area gradually decreased, but the mean gray scale gradually increased, but these changes were not evident in the sciatic nerve transection group.

Table 3 Rat gastrocnemius muscle motor end plate cross-sectional area (μm^2) and gray scale

Group	2 weeks after injury		4 weeks after injury		10 weeks after injury	
	Cross-sectional area	Gray scale	Cross-sectional area	Gray scale	Cross-sectional area	Gray scale
VRT	114.81±24.03	15.36±4.13	99.15±17.75	18.60±4.47	51.37±10.45[ab]	37.30±5.19[ab]
DRT	115.40±21.01	15.12±3.03	114.10±19.87	16.42±3.37	112.15±15.74	17.01±3.79
SNT	112.50±21.97	16.10±3.24	96.71±18.44	19.81±5.93	47.24±7.06[ab]	41.15±5.07[ab]
Control side	117.33±22.85	14.78±3.15	116.38±23.23	14.32±3.02	118.06±21.31	14.51±2.92
F	0.047	0.161	1.536	1.864	40.473	59.384
P	0.986	0.921	0.236	0.168	0.000	0.000

Data are expressed as mean ± SD of six rats from each group at each time point. The multiple-sample means were compared using analysis of variance (one-way K level), and paired comparison of means was conducted using independent two-sample t-tests. [a]$P < 0.01$, vs. control side; [b]$P < 0.01$, vs. 2 and 4 weeks after nerve injury.

VRT: Ventral root transection; DRT: dorsal root transection; SNT: sciatic nerve transection.

Results from the present study support the idea that nerves are critical for the nutrition of dominant skeletal muscle[17]. After simple motor nerve or sensory nerve injury, uninjured sensory nerves or motor nerves can provide a necessary nutritional environment for the target organ, the skeletal muscle, to delay muscle atrophy[18-19]. In addition, there are differences in the nutritional support of skeletal muscle by motor and sensory nerves. The motor nerves play a dominant role in the nutrition of skeletal muscle, exhibiting great physiological influence and important regulatory effects, while sensory nerves are not as important. Thus, after motor nerve injury or disease, the progression of disease is relatively fast compared with that after sensory nerve injury.

A previous study showed that the normal morphology and structure of muscle cells are maintained by neurotrophic factors, and that nutritional disturbance of skeletal muscle cells is the most evident change after denervation[20]. In the present study, the ultrastructure of the gastrocnemius muscle cells exhibited similar changes to those observed in other muscle cells after denervation. With prolonged injury time, mitochondrial swelling, disorderly myofilaments and sarcomeres, shortened cristae, expanded sarcoplasmic reticulum, reduced glycogen granules, and enlarged nuclei were observed. At the same time point, those changes were most evident in the sciatic nerve transection group, followed by the ventral root transection group, and then the dorsal root transection group. This directly shows the nutritional effects of motor nerves on skeletal muscle cells, as well as the harmful effects of nerve injury on skeletal muscle cells. In addition, the number of gastrocnemius muscle satellite cells increased from the second week after denervation, reached a peak value at 4 weeks, and significantly decreased at 10 weeks. The satellite cells are multipotent muscle-derived stem cells. They can differentiate into myoblasts in the presence of a specific microenvironment and regulatory factors, participating in regeneration and repair of skeletal muscle[21-23]. However, the mechanism of differentiation remains uncertain. We presume that the early increase in muscle satellite cells may be associated with stimulatory compensation after denervation[24], but they gradually die during long-term denervation and are not able to regenerate, resulting in a reduction of the number of muscle satellite cells[25-26].

The motor end plate is an effector formed from the motor neuron axonal terminal and the skeletal muscle fiber, distributing signals to the skeletal muscle to control myofibrillar contraction. Cholinergic nerves and nerve impulses can only transmit the neurotransmitter acetylcholine to the muscle through the motor end plate, to induce muscle contraction. Acetylcholinesterase has specific effects on the hydrolysis of acetylcholine and mainly exists in the motor end plate[27-28]. The normal structure and function of the motor end plate is maintained by a complete connection with neurons[29].

Studies have shown that the motor end plate area and acetylcholinesterase content can reflect the function of the motor neuron and the degeneration of the motor end plate after denervation[30-31]. In the present study, with prolonged denervation, the motor end plate area was gradually reduced and the mean gray scale increased in the ventral root transection and sciatic nerve transection groups, but remained unchaged in the dorsal root transection group. There were no significant differences in motor end plate area and gray scale after 4 weeks between the three injury groups and the control side. At 10 weeks after motor nerve injury in rats, the motor end plate area diminished and the gray scale increased, indicating that sensory nerve injury cannot induce obvious manifestations of motor end plate atrophy and does not protect the motor end plate, but that motor nerve injury induces motor end plate atrophy. The atrophy of the motor end plate is slower than the morphological changes in skeletal muscle, possibly benefiting from reversibility and nerve regeneration after skeletal muscle atrophy[32].

In conclusion, skeletal muscle function and activity depend on intact innervation. The nutritional effects of motor and sensory nerves are different. Motor nerves exhibit stronger nutritional support. Therefore, it is important to pay attention to the protection and reconstruction of motor nerves during skeletal muscle regeneration and repair, and especially to the re-innervation of motor nerves.

MATERIALS AND METHODS

Design
A randomized, controlled animal study.

Time and setting
The experiment was performed at the Laboratory of Morphology, Nantong University and the Laboratory of the Department of Orthopedics, at the Third Affiliated Hospital of Nantong University, China between July 2007 and July 2010.

Materials

A total of 54 Sprague-Dawley rats of either gender, aged 10–12 weeks, were provided by the Laboratory Animal Center of Nantong University (permission No. SCXK (Su) 2007-0021). All rats were housed with a 12 hour light-dark cycle at 22 ± 2°C and 45–55% humidity. Experimental procedures were performed in accordance with the *Guidance Suggestions for the Care and Use of Laboratory Animals*, formulated by the Ministry of Science and Technology of China[35].

Methods

Establishment of animal models

According to a method described previously[34-35], rat models of motor nerve and/or sensory nerve injury were established. The rats were weighed, followed by anesthesia by intraperitoneal injection of the anesthetic compound chlorpent (0.2 mL/100 g of a solution containing 4.25 g/mL chloral hydrate, 2.12 g/mL magnesium sulfate, 0.88 g/mL pentobarbital sodium, 14.25 mL absolute alcohol, 33.80 mL 1,2-propylene glycol, and 51.95 mL double distilled water per 100 mL). The rats were placed in a prone position and subjected to shaving, disinfection and draping.

Ventral root transection: A longitudinal medial incision was made at L_3–S_1 to expose the left lumbar vertebra from the posterior view, and the L_{4-6} nerve root was exposed following the removal of articular processes and a section of the vertebral plate (supplementary Figure 1 online). A 1 cm length of the ventral spinal nerve root was transected.

Dorsal root transection: a 1 cm length of the left L_{4-6} dorsal spinal nerve root was transected.

Sciatic nerve transection: An arc-shaped incision was made on the posterior lateral side of the left leg to expose the sciatic nerve stem 5 mm inferior to the border of the piriformis muscle. A 1 cm length of sciatic nerve was excised, and the two stumps were separately turned by 180° and fixed to the sarcolemma of the gluteus and the biceps femoris, to prevent natural growth between nerves.

The right leg gastrocnemius muscle of each rat was not treated and was used as a control.

Observation of rat behaviors

Left posterior limb appearance, movement and coordination were observed 2, 4 and 10 weeks after nerve injury. Bilateral posterior limb responses to puncture (pricking with a needle to a depth of 5 mm) were observed to evaluate nerve reaction.

Gastrocnemius muscle wet weight changes

After anesthesia, the gastrocnemius muscle from the median and lateral condyles of the femur to the calcaneal tuberosity was harvested from both legs and the wet weight (accuracy, 1/100 000 g) was weighed on a Mettler Toledo AB204-S electronic balance (Bern, Switzerland). The wet weight changes are represented as the residual muscle rate, calculated as follows: denervated gastrocnemius muscle wet weight/control gastrocnemius muscle wet weight.

Measurement of gastrocnemius muscle cell diameter and cross-sectional area

The middle-inferior muscle tissues of the gastrocnemius muscle from both sides were harvested 2, 4 and 10 weeks after nerve injury and prepared as 10 μm thick frozen sections. Following hematoxylin-eosin staining, the sections were observed under a light microscope (B204 Olympus, Tokyo, Japan) and muscle fiber equivalent circle diameter and cross-sectional area were analyzed by an imaging analyzer (Jiangsu Jeda Science-Technology Development, Jiangsu, China). Six areas were selected from each sample, and six nonoverlapping low-power fields were randomly selected from each plane (objective magnification, 10 ×, unit pixel length 0.659 3 microns/pixel). Photos were collected using an Eikon Eclipse E2000 digital camera (Olympus) and analyzed using a morphology imaging analysis system (HPIAS-1000 high definition color pathology report analysis system, Qingping Imaging, Tongji Hospital of Huazhong University of Science and Technology, Wuhan, China). The corresponding values of each muscle fiber in the field of view were measured, and the mean values were used as the equivalent cell diameter and cross-sectional area of the sample.

Measurement of gastrocnemius muscle cell ultrastructure using a transmission electron microscope

The middle-inferior tissues of the gastrocnemius muscle were harvested and chopped into 1 mm^3 blocks after removing the connective tissues. 4–6 tissue blocks from each sample were fixed successively in 2.5% glutaraldehyde and 1% osmic acid for 2 hours, dehydrated in gradient ethanol and acetone, embedded in epoxy resin Epon618, sliced, and stained with uranyl acetate-lead citrate. Cell ultrastructure of skeletal muscle after denervation was observed using

a transmission electron microscope (JEOL-100S; JEOL, Tokyo, Japan).

Observation of the gastrocnemius muscle motor end plate

The middle-inferior part of the gastrocnemius muscle tissue was fixed in 4% paraformaldehyde (pH 7.2) at 4°C overnight and subsequently transferred to 20% and 30% sucrose (pH 7.2). Following subsidence of the tissue blocks, the gastrocnemius muscle was frozen and successively cut into 15-μm thick sections at transverse and longitudinal planes, attached to 10% polylysine-precoated slides, dried at room temperature, and stained for acetylcholinesterase[38]. Finally, the cross-sectional area and the mean gray-scale of the gastrocnemius muscle motor end plate were measured using a light microscope and an imaging analyzer. Six areas were selected from each sample, and six non-overlapping low-power fields were randomly selected from each plane (objective magnification, 40 ×, unit pixel length 0.161 3 microns/pixel). Photos were collected using an Eikon Eclipse E2000 digital camera and analyzed using a morphology imaging analysis system. The corresponding values of each motor end plate in the field of view were measured, and the mean values were used as the cross-sectional area and mean gray scale of the sample.

Statistical analysis

All measurement data were statistically processed using Stata 7.0 software (Stata, College Station, TX, USA) and were expressed as mean ± SD. One-way analysis of variance and independent two-sample t-tests were used. A level of $P < 0.05$ was considered statistically significant.

Ethical approval: This study was approved by the Animal Ethics Committee, Third Affiliated Hospital of Nantong University in China.
Author statements: The manuscript is original, has not been submitted to or is not under consideration by another publication, has not been previously published in any language or any form, including electronic, and contains no disclosure of confidential information or authorship/patent application disputations.
Supplementary information: Supplementary data associated with this article can be found in the online version, by visiting www.nrronline.org.

REFERENCES

[1] Lukas TJ, Wang AL, Yuan M, et al. Early cellular signaling responses to axonal injury. Cell Commun Signal. 2009;7: 5.

[2] Singh OV, Yaster M, Xu JT, et al. Proteome of synaptosome-associated proteins in spinal cord dorsal horn after peripheral nerve injury. Proteomics. 2009;9(5): 1241-1253.

[3] Tews DS, Goebel HH, Schneider I, et al. DNA-fragmentation and expression of apoptosis-related proteins in experimentally denervated and reinnervated rat facial muscle. Neuropathol Appl Neurobiol. 1997;23(2): 141-149.

[4] Li ZB, Lehar M, Samlan R, et al. Proteomic analysis of rat laryngeal muscle following denervation. Proteomics. 2005; 5(18):4764-4776.

[5] Hart AM, Terenghi G, Wiberg M. Neuronal death after peripheral nerve injury and experimental strategies for neuroprotection. Neurol Res. 2008;30(10):999-1011.

[6] Sekiguchi M, Sekiguchi Y, Konno S, et al. Comparison of neuropathic pain and neuronal apoptosis following nerve root or spinal nerve compression. Eur Spine J. 2009; 18(12):1978-1985.

[7] Saito H, Kanje M, Dahlin LB. Delayed nerve repair increases number of caspase 3 stained Schwann cells. Neurosci Lett. 2009;456(1):30-33.

[8] Cheng FC, Tai MH, Sheu ML, et al. Enhancement of regeneration with glia cell line-derived neurotrophic factor-transduced human amniotic fluid mesenchymal stem cells after sciatic nerve crush injury. J Neurosurg. 2010;112(4):868-879.

[9] Kim JI, Choe MA. Effects of unilateral sciatic nerve injury on unaffected hindlimb muscles of rats. J Korean Acad Nurs. 2009;39(3):393-400.

[10] Batt J, Bain J, Goncalves J, et al. Differential gene expression profiling of short and long term denervated muscle. FASEB J. 2006;20(1):115-117.

[11] Jaeger MR, Braga-Silva J, Gehlen D, et al. End-to-end versus end-to-side motor and sensory neurorrhaphy in the repair of the acute muscle denervation. Ann Plast Surg. 2011;67(4):391-396.

[12] Elsohemy A, Butler R, Bain JR, et al. Sensory protection of rat muscle spindles following peripheral nerve injury and reinnervation. Plast Reconstr Surg. 2009;124(6): 1860-1868.

[13] Sun L, Wu Z, Baba M, et al. Cathepsin B-dependent motor neuron death after nerve injury in the adult mouse. Biochem Biophys Res Commun. 2010;399(3):391-395.

[14] Kanamori A, Catrinescu MM, Kanamori N, et al. Superoxide is an associated signal for apoptosis in axonal injury. Brain. 2010;133(9):2612-2625.

[15] Li XF, Xu LQ, Xi ZJ, et al. Progress of experimental study on cell apoptosis after peripheral nerve injury and the protective effect of Chinese medicine. Zhong Xi Yi Jie He Xue Bao. 2009;7(10):983-990.

[16] Sun JM, Zhao L, Jiang DL, et al. Effects of highly selective radicotomy on the structure of rat gastrocnemius muscles. Shenjing Jiepou Xue Zazhi. 2008;24(1):26-30.

[17] Wang H, Gu Y, Xu J, et al. Comparative study of different surgical procedures using sensory nerves or neurons for delaying atrophy of denervated skeletal muscle. J Hand Surg Am. 2001;26(2):326-331.

[18] Papakonstantinou KC, Kamin E, Terzis JK. Muscle preservation by prolonged sensory protection. J Reconstr Microsurg. 2002;18(3):173-184.

[19] Bain JR, Veltri KL, Chamberlain D, et al. Improved functional recovery of denervated skeletal muscle after temporary sensory nerve innervation. Neuroscience. 2001;103(2):503-510.

[20] Sunder L. Nerve Injures and THEIR REPair. London: Churchill Living Stone. 1991.

[21] Gussoni E, Soneoka Y, Strickland CD, et al. Dystrophin expression in the mdx mouse restored by stem cell transplantation. Nature. 1999;401(6751):390-394.

[22] Seale P, Rudnicki MA. A new look at the origin, function, and "stem-cell" status of muscle satellite cells. Dev Biol. 2000;218(2):115-124.

[23] Jackson KA, Mi T, Goodell MA. Hematopoietic potential of stem cells isolated from murine skeletal muscle. Proc Natl Acad Sci U S A. 1999;96(25):14482-14486.

[24] Wu J, Sun XJ, Zhong SZ, et al. Changes in muscle satellite cells in denervated and innervated muscles. Zhongguo Xiufu Chongjian Waike Zazhi. 2006;20(10): 1047-1051.

[25] Zhao ZG, Liu Q, Li G. The effect of transplantation of skeletal muscle satellite cell on retard the denervated muscles atrophy. Zhonghua Guke Zazhi. 2006;26(1): 51-55.

[26] Viguie CA, Lu DX, Huang SK, et al. Quantitative study of the effects of long-term denervation on the extensor digitorum longus muscle of the rat. Anat Rec. 1997; 248(3):346-354.

[27] Inestrosa NC, Perelman A. Distribution and anchoring of molecular forms of acetylcholinesterase. Trends Pharmacol Sci. 1989;10(8):325-329.

[28] Legay C. Why so many forms of acetylcholinesterase? Microsc Res Tech. 2000;49(1):56-72.

[29] Rantanen J, Ranne J, Hurme T, et al. Denervated segments of injured skeletal muscle fibers are reinnervated by newly formed neuromuscular junctions. J Neuropathol Exp Neurol. 1995;54(2):188-194.

[30] Fawcett JW, Keynes RJ. Peripheral nerve regeneration. Annu Rev Neurosci. 1990;13:43-60.

[31] Xu JG, Gu YD. Experimental study of morphology and electrophysiology on denervated skeletal muscle. Zhongguo Xiufu Chongjian Waike Zazhi. 1999;13(4): 202-205.

[32] Williams AH, Valdez G, Moresi V, et al. MicroRNA-206 delays ALS progression and promotes regeneration of neuromuscular synapses in mice. Science. 2009; 326(5959):1549-1554.

[33] The Ministry of Science and Technology of the People's Republic of China. Guidance Suggestions for the Care and Use of Laboratory Animals. 2006-09-30.

[34] Schaeffer V, Meyer L, Patte-Mensah C, et al. Sciatic nerve injury induces apoptosis of dorsal root ganglion satellite glial cells and selectively modifies neurosteroidogenesis in sensory neurons. Glia. 2010;58(2):169-180.

[35] Atlasi MA, Mehdizadeh M, Bahadori MH, et al. Morphological identification of cell death in dorsal root ganglion neurons following peripheral nerve injury and repair in adult rat. Iran Biomed J. 2009;13(2):65-72.

[36] Mitchell SJ, Rawlins JN, Steward O, et al. Medial septal area lesions disrupt theta rhythm and cholinergic staining in medial entorhinal cortex and produce impaired radial arm maze behavior in rats. J Neurosci. 1982;2(3): 292-302.

(Edited by Jiang XM, Chen TY/Su LL/Song LP)